BOLETIN DE LA SOCIEDAD ESPAÑOLA DE
Cerámica y Vidrio
www.elsevier.es/bsecv

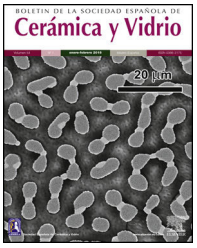

Original

Elaboration of a high mechanical performance refractory from halloysite and recycled alumina

Abdelilah El Haddar[a,b,*], *Ahmed Manni*[c], *Ali Azdimousa*[a], *Iz-Eddine El Amrani El Hassani*[b], *Abdelilah Bellil*[b], *Chaouki Sadik*[c], *Nathalie Fagel*[d], *Meriam El Ouahabi*[d]

[a] *Laboratory of Applied Geosciences, Faculty of Sciences, University of Mohammed 1, Oujda, Morocco*
[b] *Geomaterial & Geoenvironment Team, GEOPAC Centrer, Scientific Institute, Mohammed V, University of Rabat, Morocco*
[c] *Laboratory of Physical Chemistry of Applied Materials (LPCMA), Department of Chemistry, Faculty of Sciences Ben Msik, Hassan II University, Morocco*
[d] *U.R. Argile, Géochimie et Environnement sédimentaires (AGEs), Département de Géologie, Quartier Agora, Bâtiment B18, Allée du six Août, 14, Sart-Tilman, Université de Liège B-4000, Belgium*

ARTICLE INFO

Article history:
Received 11 March 2019
Accepted 1 August 2019
Available online 19 August 2019

Keywords:
Halloysite
Silica-alumina refractory
Ceramic aggregate
Mechanical properties
North Eastern Rif (Morocco)

ABSTRACT

The present study is a contribution to the valorization of halloysite clay from North Eastern Rif (Nador, Morocco) in the field of Silica-alumina refractory. For this purpose, six mixtures (M1–M6) were tested using marl, diatomite and silica sand aggregates in order to enhance halloysite performances, and to develop high temperature ceramic up to 1300 °C (silico-aluminous refractory "S-Al-R"). Among all the mixtures tested, the mixture M6 provides good technical quality: Porosity (P) = 21.75%; density (*d*) = 1.94 g/cm^3; thermal shrinkage (R) = 2.7% and flexural strength (Rf) = 29.05 MPa. Addition to the mixture (M6) of 25% of the recycled alumina "Rec-Al", obtained from silico-aluminous refractory bricks waste, has substantially strengthened the mechanical performance of the silico-aluminous refractory (Rf = 45.08 MPa).

Halloysita y alúmina reciclada para un alto rendimiento mecánico refractario

Palabras clave:
Halloysita
Refractario de sílice-alúmina
Agregados de cerámicas
Rendimiento mecánico
Noreste del Rif (Marruecos)

RESUMEN

El presente estudio es una contribución a la valorización de la halloysita del noreste del Rif (Nador, Marruecos) en el campo de los refractarios de sílice-alúmina. Para este propósito se experimentaron seis mezclas (M1 a M6) usando agregados de arena de marga, diatomita y sílice para mejorar el rendimiento de las instalaciones y desarrollar cerámicas de alta temperatura hasta 1300 °C (refractarios sillico-aluminosos «S-Al-R»). Entre todas las mezclas experimentadas, la mezcla M6 proporciona una buena calidad técnica: porosidad

* *Corresponding author.*
E-mail address: el.haddar.abdelilah@gmail.com (A. El Haddar).
https://doi.org/10.1016/j.bsecv.2019.08.002

(P) = 21.75%; densidad (d) = 1.94 g/cm^3; contracción térmica (R) = 2.7% y resistencia a la flexión (Rf) = 29.05 MPa. La adición a la mezcla (M6) del 25% de la alúmina reciclada «Rec-Al», obtenida a partir de residuos de ladrillos refractarios sillico-aluminosos, ha fortalecido sustancialmente el rendimiento mecánico del producto refractario «M6» (Rf = 45.08 MPa).

Introduction

Faced with the growing developments and numerous innovations that are appearing in ceramic industry, in particular refractory retains the largest shares of ceramics market worldwide. The strategic importance of these materials is considerable, they respond to a real demand of four important economic sectors [1]: (1) traditional materials of high temperature, such as metallurgy, glass and ceramics. Notably, iron and steel alone represent about 60% of the used materials; (2) environment sector, principally in the field of waste recycling and energy recovery; (3) petrochemistry and emerging biofuels sector of 2nd generation through thermo-chemical processes; (4) clean energy and electricity production, such as hydrogen production or new generation of nuclear power plants (EPR generation IV).

In recent decades, several works have been done on refractory materials and their applications [2–19]. Based on their chemical and mineralogical nature, refractories are divided into three categories: (1) silico-aluminous refractories, which range from pure silica to pure alumina, in order of increase alumina and decrease silica contents; (2) basic refractories, consisting of simple or combined basic oxides (magnesia, lime, chromium oxide, dolomite and forsterite); (3) special refractories that correspond to particular uses (e.g. construction of crucible, some parts of furnaces).They include materials like pure alumina, sialons (Si—Al—O—N), thoria (ThO_2), beryllia (BeO), zirconia, boron nitride, carbon, carbides and spinel.

In this work we are interested in the acid refractories (silico-aluminous system). In Morocco, and more particularly in the North-Eastern Rif (Fig. 1), a wide range of geomaterials deposits are available (e.g. volcanic, metamorphic, and sedimentary). Among them, we selected and characterized essentially mineral substances having a high silico-aluminous amount (Fig. 1) favorable for refractory ceramic. Clayey raw material consists of halloysite, which is the most frequently used for refractory manufacture, due to its high alumina content. Moreover, this raw halloysite has shown a relatively high shrinkage of around 7.5% and a crack development at 1100 °C [20]. The reason why appropriates formulations must be made in order to avoid any manufacturing defects. It is recognized that the performance of a refractory material is directly related to its texture and richness in refractory minerals such as mullite, corundum, periclase, spinel and alumina [21–26]. Marl, diatomite and silica sand, have been successfully used as aggregates to improve technical quality of ceramic products [18,27–29].

The silico-aluminous refractories are based on synthesis of mullite, by the reaction of silica and alumina oxides at temperature higher than 1200 °C. In the absence of natural alumina-rich mineral substances (bauxites) in Morocco [7], we have tried to enhance strangeness of halloysite by recycled alumina (Rec-Al) from former aluminous refractory. The reuse of waste from silico-aluminous refractory brick permit to eliminate some waste by recycling and help to solve problems related to the lack of aluminous raw materials.

The objective of this work is to develop refractory bricks based on raw halloysite mixed with silico-aluminous mineral aggregates and improved with the addition of recycled alumina (Rec-Al).

Materials and experimental procedures

Materials

Halloysite

The halloysite deposit is located in the southern part of the Neogene basin of Melilla (NE Morocco), at the foot of the Gourougou volcano, in the Maaza valley (x: 35°16′43.751″ y: 3°01′20.865″) (Fig. 1). White layer of halloysite, of 25–130 cm thick (Fig. 2a), occurred in wedge-shaped form in contact with lower reef limestone and upper volcanic sand, associated with a gray-colored alunite [20,34].

Marl

The raw marl is originating from the Molay Rachid basin, situated at 30 km SE from the city of Nador (x: 35°16′43.751″ y: 3°01′20.865″)(Fig. 1). This marl corresponds to marine deposit of late Miocene age. The sediment is very fine grain, gray and friable, which changes to a, yellowish or greenish color toward the upper level. This material is currently exploited locally for brick manufacture (Fig. 2b).

Diatomite

Diatomite deposit is located in the north-western part of the Neogene Boudinar basin (Morocco, North-East Rif) (x: 35°11′22.20″N; y: 03°37′52.74O), at the foot of the Ras Tarf volcano (Figs. 1 and 2c) in the area of Sidi Haj Youssef (SHY). According to Hilali et al. [34], this diatomite outcrop extends over 2 km^2, surrounded by a large W–E fault on West and East, and the Tighza River on South-East. The diatomite is present in foliated layers, white, brownish or grayish, light and fine grained. The deposit consists of six layers of diatomite, separated by grayish-blue argillites, with a slight dip toward the SE.

Silica sand

The silica sand material is from an artisanal quarry situated 3 km SE of the Mechraa Hammadi Dam (x: 34°42′56.94″N; y: 02°47′14.27O) (Figs. 1 and 2d). The deposit shows a pink-white

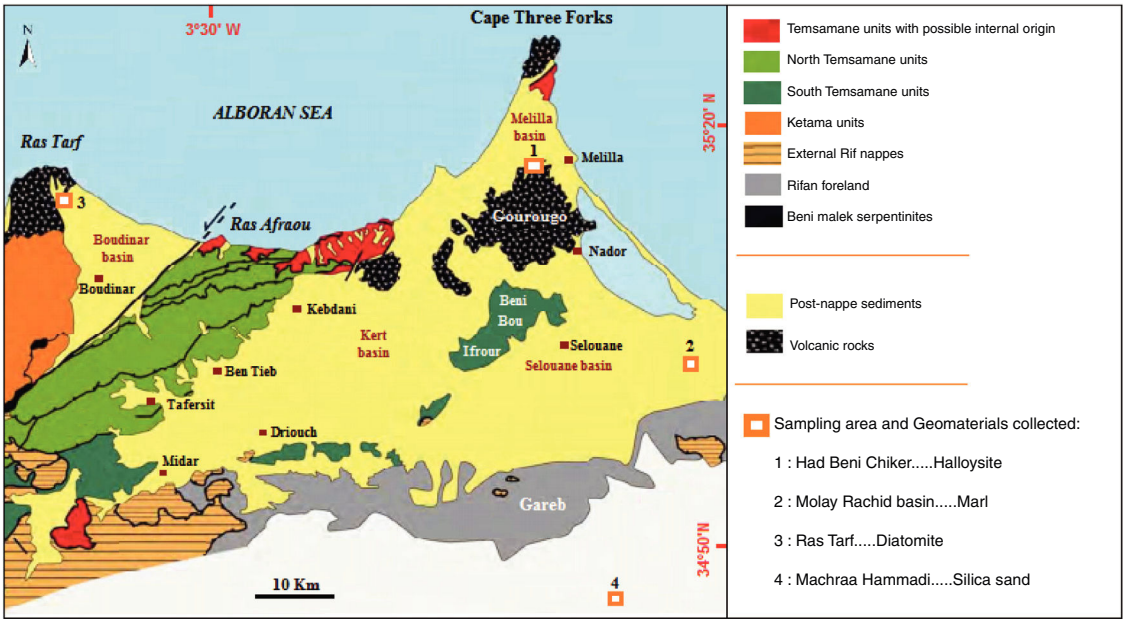

Fig. 1 – Geological context of the study area, based on a synthesis of geological maps of the north-eastern Rif [30–33].

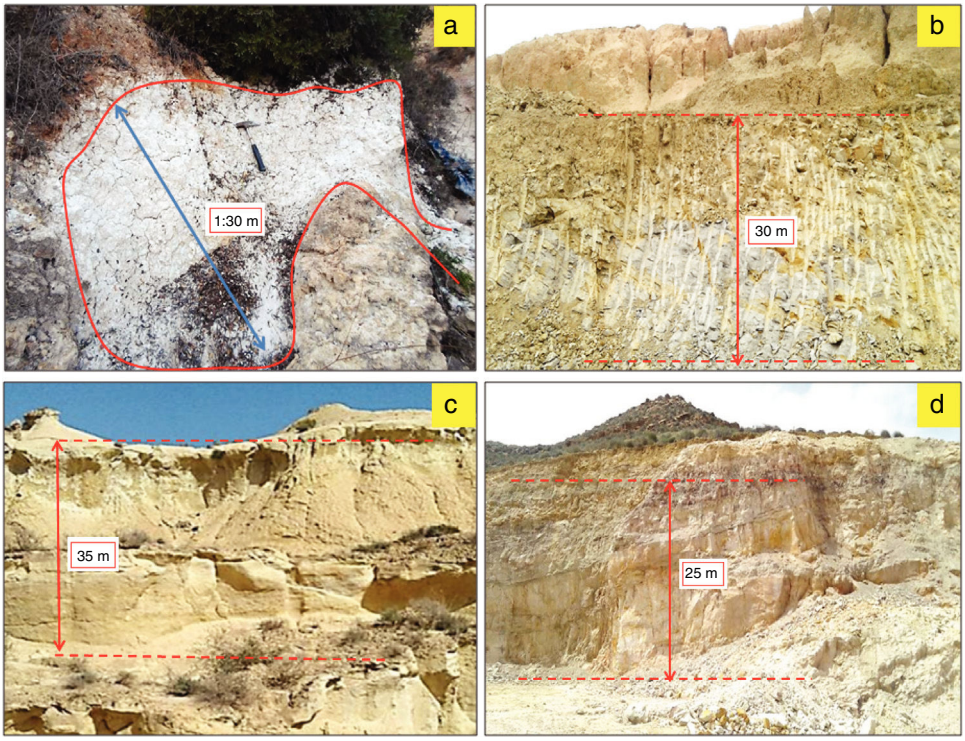

Fig. 2 – Outcrops of the studied deposits facies. (a) White halloysite deposit of the Neogene Melilla basin, (b) Gray yellow marly clay deposit of the Miocene Molay Rachid basin, (c) white, brownish or grayish diatomite deposit of the Neogene Boudinar basin, (d) pink-white silica sand deposit of Mechraa Hammadi.

facies of up to 200 m-thick and belongs to the Beni Snassen Massif [35]. The exploitable sand is found in shallow layers intercalated with marl levels of late Jurassic age. The sand is coarse (0.1–0.4 mm), composed of limpid quartz with smooth surface [7,36].

Recycled refractory brick waste

Silico-aluminous refractory brick waste (Rec-Al) used as coatings in furnaces of ceramic or steel industry is reused in this study as an additive to enhance technological properties of raw halloysite. These bricks served as coatings in furnaces for

a short period of 3 years and thus present low level of contamination. The waste of refractory brick is finely grounded (<100 μm) and added in the mixture as supplement of alumina.

Experimental procedures

Mineralogical and chemical analysis

The mineralogical composition was identified by X-ray diffraction (XRD) using a powder Brucker D8-Advance diffractometer (University of Liege, Belgium) operating at 40 kV and 25 mA using Cu-Kα1 radiation (λ = 1.5406 Å). For the analysis of the total disoriented powder 1 g of the sample was sieved to 250 μm and placed on a sample holder and then gently compacted in order to limit any preferential orientation of minerals. The relative abundance of minerals has been estimated semi-quantitatively (± 5%) from the height of the main peak multiplied by correction factors [37,38]. The clay mineralogy was determined on oriented mounts [39] prepared from the < 2 mm fractions obtained by dispersion in distilled water of 1 g of the bulk sample. The suspension was first sieved at 63 μm to limit particle settling during decantation and to reduce the amount of impurities in the clay aggregates. The <2 μm fraction was taken from the suspension according to Stoke's law, placed on a glass slide. The oriented aggregates were subjected to three successive treatments, air drying, ethylene glycol (EG) solvation and heating at 500 °C for 4 h, to identify the minerals of the clay-size fraction. Qualitative identification was performed by referring to the interlayer space [40] and the values of the intensity of the main reflections between the three X-ray patterns, characteristic of each mineral. Semi-quantitative estimation of clay minerals is based on the height of specific reflections measured in general in the Ethylene glycol runs, multiplied by corrective factors [41]. The carbonate ($CaCO_3$) content in the samples was measured using a Bernard calcimeter, on the basis of the volumetric analysis of the CO_2 liberated during hydrochloric acid leaching. The chemical composition of major elements was determined by X-Ray Fluorescence spectroscopy (XRF) with a Panalytical Axios spectrometer equipped with Rh-tube, using argon-methane gas. Data handling was performed with the IQ + software (University of Liege, Belgium).

Ceramic properties

Preparation and mix proportioning. The materials studied were dried at 100 °C in the oven. Then, they were finely ground (mean grain size < 100 μm) using a planetary ball mill (PM100, Retsch, Germany). Samples were placed on a tungsten carbide jar with a holding capacity of 250 mL containing seven tungsten carbide balls (d = 15 mm) at a speed of 350 rpm. Six mixtures were performed (M1–M6) according the proportions reported in Table 3. It is noted that each mixture contained a considerable quantity of material ~100 g, enough to manufacture ceramic bodies in the form of a rectangular briquettes with 10 cm × 5 cm × 1 cm of average size. The mixtures prepared were wetted at 7 wt.% and then homogenized and sieved with a 100 μm mesh. The powdered mixtures were uniaxially compacted using hydraulic press under a pressure of 30 MPa. The bodies obtained were dried in the open air for 24 h and afterward in the oven at 110 °C for 24 h. Then, they were fired in an electric furnace (Thermolyne 46200) in an oxidizing atmosphere following two different temperatures steps: from room temperature up to 600 °C with heating rate of 3 °C/min during 30 min. From 600 °C to 1300 °C with heating rate of 3 °C/min for 30 min. After firing at 1300 °C, the furnace was cooled down to room temperature with cooling rate of 5 °C/min. The process was repeated for sintering at 1500 °C using the same procedure. Three replicate bricks were tested for each mixture and the average values were taken.

Technological test

Fired products were characterized to determine their mechanical properties like flexural strengths with three-point bending. This test was carried out at ambient temperature. The loading procedure consisted of applying a preliminary load (0.05 kN) at a rate of 0.5 mm/min to eliminate positioning defects of the specimens. The distance between bottom supports was 80 mm.

The determination of the value of shrinkage was done by the measurement of the variation of the average lengths of the lines recorded on briquettes between drying at 110 °C and firing at 1300 and 1500 °C. The following formula allows the calculation of the firing shrinkage: Shrinkage (%) = (L110 − Lt/L110) × 100, where Lt is the length after firing, and L110 the length after drying at 110 °C. The water absorption, bulk density and apparent porosity were measured according to ASTM norm [42].

As the major properties of the refractory materials are intimately connected to their mineralogical composition, the samples were finely crushed and analyzed by X-ray diffraction. The different phases formed after firing at 1300 and 1500 °C were identified using the X'PertHighScore Plus software. The samples microstructure was evaluated using scanning electron (SEM) and polarized microscope (using both natural light "AL" and polarized light "APL"). For this latter, we started by making thin slices approximately 30 μm thick in brick fragments fired at 1500 °C. These thin sections have been observed under a microscope Olympus BX 51TF (Scientific Institute, Rabat). Scanning electron microscopy (SEM) images were obtained on the refractory product with a Philips XL30 SEM (University of Liege, Belgium). Phase identification of the ceramic refractory was also performed by dispersive X-ray spectroscopy (EDX). The images were obtained with a secondary electron detector at 10 kV. The <250 mm fraction was dispersed over a sample holder and gold-sputtered for (EDX) analysis.

Results and discussion

Mineralogical and chemical analysis

Mineralogical composition (XRD) and carbonate contents of the raw materials (halloysite, diatomite, marl, sand silica and recycled alumina (Rec-Al) are showed in Table 1.

The halloysite consists mainly of 7 Å non-hydrated halloysite (68% of metahalloysite) and traces of smectite and illite. It occurs in association with gibbsite, alunite, K-feldspar and other minor phases (tridymite, fluorite and halite). The marl is characterized by predominance of kaolinite (21%), illite (20%), quartz (18%), calcite (18%), and small amounts of feldspar,

Table 1 – Quantitative mineralogical composition (XRD) of crystalline and amorphous phases, and carbonate content (Bernard Calcimeter) of studied raw materials.

	Halloysite (%)	Marl (%)	Diatomite (%)	Silica sand (%)	Rec-Al (%)
Amorphous phase	18	8	63	–	19
Crystalline phase	82	92	37	100	81
Quartz	–	18	24	93	–
K-Feldspar	10	2	–	–	–
Plagioclase	–	6	6	–	–
Calcite	–	18	26	–	–
Dolomite	–	7	12	–	–
Mullite	–	–	–	–	85
Diopside	2	–	–	–	–
Gibbsite	3	–	–	–	–
Hematite	–	3	–	4	–
Cristobalite	–	–	–	–	15
Tridymite	6	–	–	–	–
Alunite	1	–	–	–	–
Fluorite	4	–	–	–	–
Halite	1	–	–	–	–
Magnetite	–	–	–	1	–
Anatase	–	–	–	2	–
Kaolinite		21	1	–	–
Halloysite	68	–	–	–	–
Illite	4	20	9	–	–
Chlorite	–	5	–	–	–
Smectite	1	–	22	–	–
$CaCO_3$	–	16	23.5	–	–

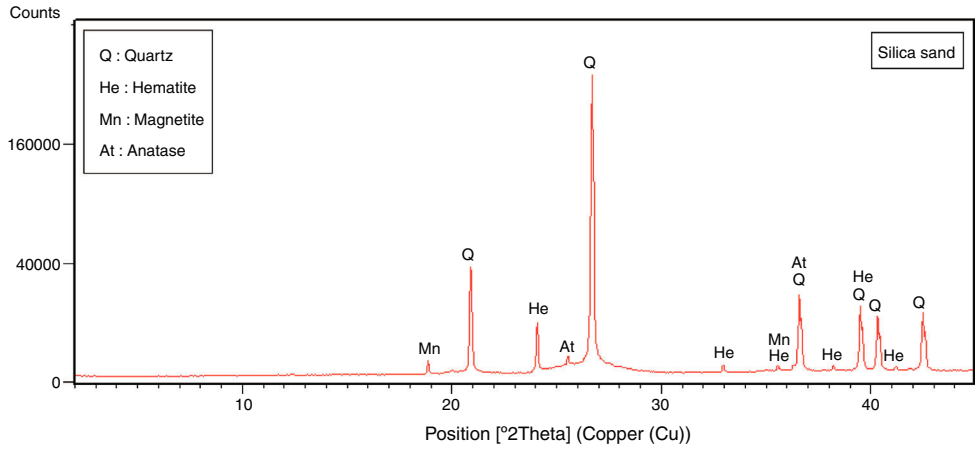

Fig. 3 – XRD spectra of silicas and from Mechraa Hammadi quarry.

dolomite, hematite and chlorite. The diatomite mostly contains calcite (26%), quartz (24%), smectite (22%) and dolomite (12%), with small amount of illite and feldspar. For the silica sand, quartz is the major mineral (93%) as shown in Fig. 3. Whereas, the recycled alumina (Rec-Al) is mainly composed of mullite (71%, Fig. 4). Contents of carbonate ($CaCO_3$) are moderate in marl (16%) and high in diatomite (23%).

The chemical compositions of raw materials, performed by X-Ray Fluorescence (XRF), are reported in Table 2. The most abundant oxide is SiO_2, which is the highest in sand silica (96.1%) and diatomite (71.5%). The highest value of Al_2O_3 is recorded for recycled brick (65.13%) and halloysite (37.4%). Marl is characterized by relatively high contents of iron (Fe_2O_3 = 10.71%).

Ceramic properties of silico-aluminous refractory "S-Al-R"

In this study, refractoriness corresponds to melting point. Halloysite has good properties for refractory ceramic. However, correction with other components is required for avoiding cracks development during firing, and also to minimize its shrinkage during sintering [20]. For this reason, six mixtures (M1–M6, Table 3) were used to manufacture ceramic bodies well stabilized and resisting to high temperature at 1300 °C (silico-aluminous refractory "S.Al.R"). Technological properties of fired samples are reported in Table 4. The results show significant fluctuations which confirm the close relationship between the composition of the raw materials and the quality of the finished ceramic product.The sintered bodies

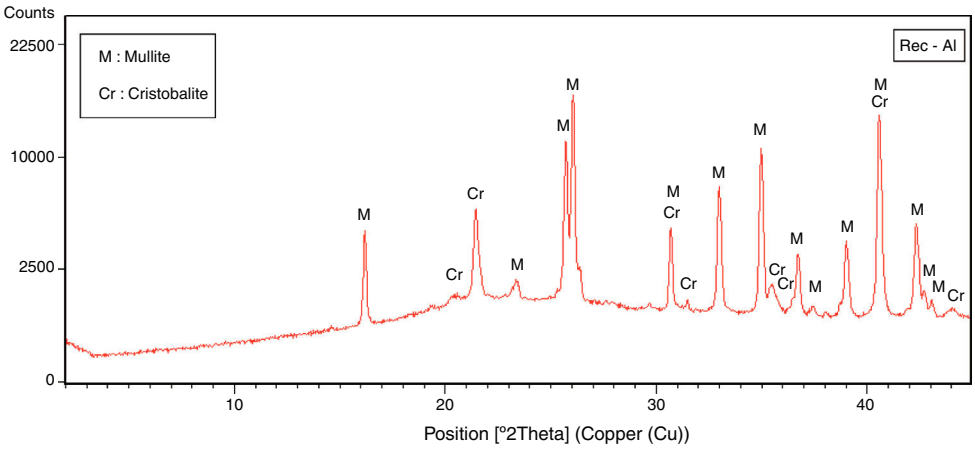

Fig. 4 – XRD spectra of waste recycled refractory used in this study (Rec-Al).

Table 2 – Chemical compositions (XRF) of the geomaterials used in this study (wt.%).

	Halloysite	Marl	Diatomite	Silica sand	Rec-Al
SiO_2	37.0	43.44	71.5	96.06	28.25
Al_2O_3	37.4	13.07	5.28	2.22	65.13
TiO_2	0.1	0.67	0.12	0.15	1.02
Fe_2O_3	0.5	10.71	2.05	0.51	2.04
CaO	0.6	8.68	9.21	0.09	0.98
MgO	1.0	2.66	1.23	0.17	–
K_2O	0.5	1.43	0.57	0.20	1.83
Na_2O	1.9	1.89	1.34	0.06	–
SO_3	1.6	0.36	0.03	–	–
MnO_2	–	0.40	–	–	–
P_2O_5	–	0.28	0.04	0.02	–
L.O.I	18	17.31	8.61	0.49	0.24
Total	98.6	99.99	99.98	99.97	99.49

Table 3 – Composition of different mixtures of halloysite with marl, diatomiteand silica sand.

Mixtures	Halloysite (%)	Marl (%)	Diatomite (%)	Silica sand (%)
M1	65	–	–	35
M2	80	–	20	–
M3	80	20	–	–
M4	50	–	25	25
M5	50	25	–	25
M6	50	25	5	20

M3 and M6 significantly have a greater flexural strength compared with others (M1, M2 and M4). The low values of firing shrinkage were observed for M1 (2%), M6 (2.7%) and M5 (3.8%), and more important values are showed for M4 (5%), M3 (6.92%) and M2 (9.85%). This relatively high shrinkage can be explained by the presence of a high amount of clay mineral, low amount of degreaser (sand) and the presence of alkaline and alkaline earths elements in raw materials. Kaolin clay (halloysite) and marl are known for their high plasticity, while, the diatomite material ($SiO_2 > 70\%$) contributes to the glassy phase formation during sintering. The consequence of glassy phase formation is the increase in firing shrinkage. The addition of 20–25% of sand fraction in the mixtures M4, M5 and M6 decreases the firing shrinkage to 5%, 3.8% and 2.7% respectively. The large values of water absorption (13.07% and 13.51%), and porosity (27.96% and 28.02%) were observed for M1 and M4 respectively. The increase in these parameters is due to the presence of a large amount of quartz. In addition, $CaCO_3$ present in diatomite and marl, begins to decompose to CaO at 700 °C, this decomposition during firing is often accompanied by the release of CO_2 outside the fired samples tending to create porous structure.

According to the results, the mixture M6 (50% halloysite + 25% marl + 5% diatomite + 20% silica) is the most optimal silico-aluminous refractory ("S-Al-R"), resisting to firing temperature that exceeds 1300 °C. This mixture (M6) has a lower linear shrinkage firing (2.7%) and a flexural strength

Table 4 – Technological properties of the fired specimens at 1300 °C/30 min.

	Shrinkage (%)	Flexural strength (MPa)	Porosity (%)	Absorption (%)	Density (g/cm^3)
M1	2	18.88	27.96	13.07	1.84
M2	9.85	25.78	22.94	9.27	1.93
M3	6.92	29.96	20.66	7.74	1.97
M4	5	21.38	28.02	13.51	1.81
M5	3.8	25.22	22.59	9.14	1.92
M6	2.7	29.05	21.75	8.22	1.94
Max	9.85	29.96	28.02	13.51	1.97
Min	2	18.88	20.66	7.74	1.81
Average	5.05	25.05	23.99	10.16	1.90

Fig. 5 – Macroscopic aspect of the briquette ceramic obtained from mixture M6 with 25% of Rec-Al, fired at 1500 °C.

equal to 29.05 MPa. Furthermore, it shows a straight edge without shape defects (e.g. cracks, distortion).

Effect of recycled refractory brick waste "Rec-Al"

In this study and by reference of a previous research [7], we have added 25% of Rec-Al in silico-aluminous refractory (M6). Thus, we have noted a very interesting improving the quality of the refractory obtained. This incorporation of alumina brick waste allows increasing the flexural strength to 45.08 MPa. These properties are essentially due to the high amount of mullite contained in the refractory brick waste (Fig. 4). The sintered bodies at 1500 °C, are of good quality, without any

Table 5 – Optimal technological results obtained for the fired specimen M6with Rec-Al at 1500 °C.

Physical properties	M6 + 25% Rec-Al
Shrinkage (%) [45]	2.1
Flexural strength (MPa) [44]	45.08
Apparent porosity (%) [42]	22.85
Water absorption (%) [42]	11.53
Bulk density (g/cm^3) [42]	1.98

Table 6 – Quantitative mineralogical composition % (XRD) of M6 fired at 1300 °C and M6 + 25% Rec-Al fired at 1500 °C.

Mineral phases (%)	M6(1300 °C)	M6 + 25% Rec-Al (1500 °C)
Mullite	27	32
Cristobalite	10	12
Quartz	32	19
Anorthite	5	–
Amorphous	26	37

cracks and surface damage, no deformation and especially a very small shrinkage 2.1% is showed (Fig. 5, Table 5).

The observations on the polarized microscope of the fired specimen at 1500 °C (Fig. 6) show that the studied material appears heterogeneous with some anisotropic crystals of quartz, amorphous zones and porosity. Quartz crystals are xenomorphic and show recognizable by their hue of polarization and their gradual extinction.

SEM images and associated EDX spectra (Fig. 7) show the presence of mullite (rich in alumina) in the form of entangled needles and bounded by a large amount of amorphous phase (37%, Table 6), supporting the refractory character of the mixture. This morphology and disposition of the mullite grains are advantageous to enhance mechanical strength. It is observed that the obtained refractory contains significant pores which have irregular shapes and sizes and randomly distributed throughout the mass of the material. This is caused by the shaping operation, the release of moisture, decomposition of $CaCO_3$, presence of inert materials (quartz and Rec-Al) inside the structure and binder structure water during firing.

The X-ray diffraction pattern (Fig. 8b) evidences the presence of mullite, quartz, small amount of cristobalite and vitreous phase (large background between $2\theta = 15°$ and $2\theta = 30°$).

The increasing firing temperature from 1300 °C to 1500 °C (Fig. 8) is marked by a decrease in the intensity of the quartz peak and the disappearance of anorthite. This is explained

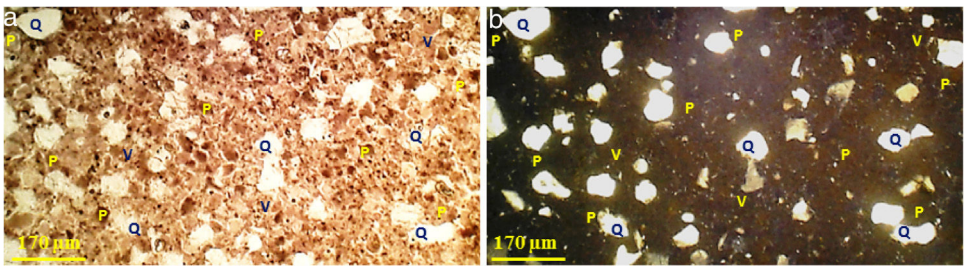

Fig. 6 – Micrography of the fired refractory specimenM6 mixed with 25% of Rec-Al at 1500 °C. () Natural microscopy light (AL). (b) Polarized microscopy light (APL). P: Porosity, Q: Quartz, V: Vitreous phase.

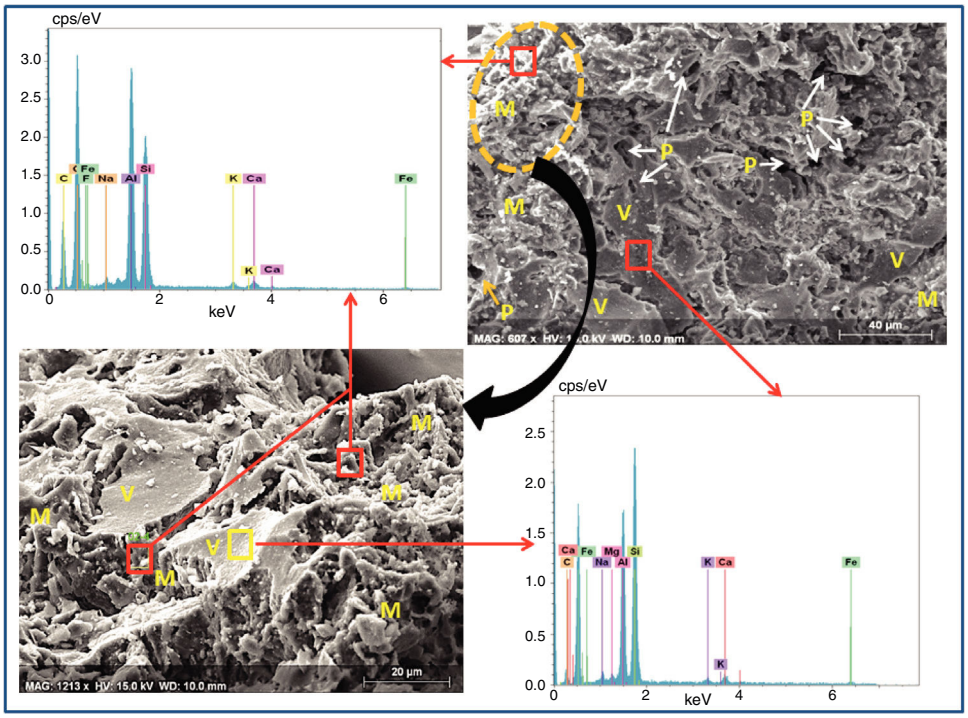

Fig. 7 – SEM images of the fired specimen of sample M6 mixed with 25% of Rec-Al at 1500 °C a and associated EDS spectra. P: Porosity, V: Vitreous phase, M: Mullite.

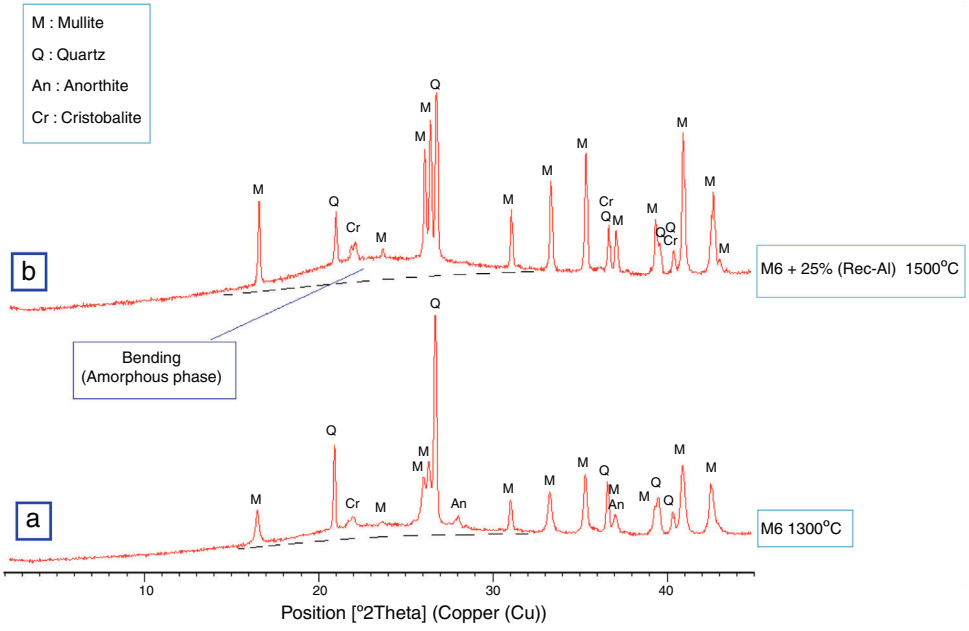

Fig. 8 – XRD spectra of sample M6 fired at 1300 °C (a), and sample M6 mixed with 25% of Rec-Al fired at 1500 °C (b).

by partial dissolution of amorphous phase content, which become diffuse (bending). The considerable development of mullite crystals is expressed by the increase in its peaks intensities (Fig. 8, Table 6). Pores still occur with irregular shapes and sizes due mainly to CO_2 release from the decomposition of plagioclase (anorthite). The free CaO would react with the silico-aluminous matrix.

Conclusion

The results of this study confirm the close relationship existing between the composition of raw materials and the quality of the ceramic products. The use of well selected mineral aggregates, contributes to enhance halloysite properties and leads to a marked improvement in the quality of the ceramic

product, through a reduction on their firing shrinkage and an increase of flexural strength. The use of marl, diatomite and silica sand as mineral adjuvants with halloysite with well-defined proportion give ceramic of good quality. Thus, the formula of mixture M6 (50% halloysite + 25% marl + 5% diatomite + 20% silica sand), gives already a good ceramic: resisting to a temperature exceeding 1300 °C, has low linear shrinkage firing (2.7%), no cracks were observed on the faces, the edges remained straight, the flexural strength is equal to 29.05 MPa and is rich in mullite. Technological characteristics of these ceramic are very interesting to justify the use of this formula as silico-aluminous refractory (S-Al-R).

Addition of 25% of Rec-Al powder to S-Al-R gives a new composition very improved. Firing shrinkage decreased from 2.7 to 2.1%. The flexural strength has increased from 29.05 to 45.08 MPa, as well as firing temperature increased from 1300 to 1500 °C. The result of this study corroborates previous work on silico-aluminous refractory by Sadik et al., 2013 [43] and shows that the addition of aluminous refractory waste, rich in mullite, allows both to obtain a high mechanical high performance refractory while solving a problem of solid waste storage.

Acknowledgments

This study was conducted in the laboratory of Geomaterials and Geoenvironment (Geo M&E) of the Scientific Institute, University Mohammed V-Agdal, Rabat, Morocco, and UR. Argile, Géochimie et Environnement sédimentaires (AGEs), Department of Geology, University of Liège, B-4000, Belgium. This research was also supported by Erasmus grants from the University of Liège, Belgium.

REFERENCES

[1] J. Poirier, Les céramiques réfractaires de l'élaboration aux propriétés d'emploi, Ver, Céram. Comp. 1 (N1) (2011).
[2] M.M. Abou-Sekkina, S.A. Abo-El-Enein, N.M. Khalil, O.A. Shalma, Phase composition of bauxite-based refractory castables, Ceram. Int. 37 (2011) 411–418.
[3] B. Amrane, E. Ouedraogo, B. Mamen, S. Djaknoun, N. Mesrati, Experimental study of the thermo-mechanical behaviour of alumina-silicate refractory materials based on a mixture of Algerian kaolinitic clays, Ceram. Int. 37 (2011) 3217–3227.
[4] C.N. Djangang, A. Elimbi, U.C. Melo, G.L. Lecomte, C. Nkoumbou, J. Soro, J.P. Bonnet, P. Blanchart, D. Njopwouo, Sintering of clay-chamotte ceramic composites for refractory bricks, Ceram. Int. 34 (2008) 1207–1213.
[5] I.D. Katsavou, M.K. Krokida, I.C. Ziomas, Determination of mechanical properties and thermal treatment behavior of alumina-based refractories, Ceram. Int. 38 (2012) 5747–5756.
[6] B.M. Kim, Y.K. Cho, S.Y. Yoon, R. Stevens, H.C. Park, Mullite whiskers derived from kaolin, Ceram. Int. 35 (2009) 579–583.
[7] C. Sadik, I.-E. El Amrani, A. Albizane, Effect of andalusite rich schist grain size and the addition of metallic aluminum powder on the properties of silica–alumina refractory, J. Asian Ceram. 1 (2013) 351–355.
[8] M. Sutcu, S. Akkurt, A. Bayram, U. Uluca, Production of anorthite refractory insulating firebrick from mixtures of clay and recycled paper waste with sawdust addition, Ceram. Int. 38 (2012) 1033–1041.
[9] C. Sadik, A. Albizane, I.-E. El Amrani, Production of porous firebrick from mixtures of clay and recycled refractory waste with expanded perlite addition, J. Mater. Environ. Sci. 4 (2013) 981–986.
[10] I.V. Belyaev, A.V. Stepnov, A.V. Kireev, A.A. Pavlov, Refractory ceramic products from pure oxides with getter coatings, Refract. Ind. Ceram. 58 (2018) 615–617.
[11] P. Tofel, Evaluation of properties of newly developed refractory materials produced in SEEIF ceramic, a.s., Interceram – Int. Ceram. Rev. 65 (2016) 8–11.
[12] A.A. Biryukova, T.D. Dzhienalyev, T.A. Tikhonova, Ceramic proppants based on kazakhstan natural alumosilicate resources, Refract. Ind. Ceram. 58 (2017) 269–275.
[13] P.M. Pletnev, V.M. Pogrebenkov, V.I. Vereshchagin, D.S. Tyul'kin, Corundum refractory material in alumina-binder resistant to high-temperature deformation, Refract. Ind. Ceram. 59 (2018) 85–90.
[14] L. Yuan, Z. Yan, X. Zhang, J. Yu, Effects of SiC on the properties and microstructures of closed-pore Al_2O_3–$MgAl_2O_4$ refractory aggregates, Interceram. – Int. Ceram. Rev. 65 (2016) 50–53.
[15] S.E. Kalakhi, A. Samdi, R. Moussa, M. Gomina, Production of corundum-mullite mixture with high added value from raw materials of Morocco, New J. Glas. Ceram. 06 (03) (2016) 9.
[16] A. Sedaghat, E. Taheri-Nassaj, G.D. Soraru, T. Ebadzadeh, Retracted "Microstructure development and phase evolution of alumina–mullite nanocomposite" [Ceram. Int. 40(2) (2014) 2605–2611], Ceram. Int. 40 (2014) 16841.
[17] S. Sembiring, W. Simanjuntak, P. Manurung, D. Asmi, I.M. Low, Synthesis and characterisation of gel-derived mullite precursors from rice husk silica, Ceram. Int. 40 (2014) 7067–7072.
[18] C. Sadik, I.-E. El Amrani, A. Albizane, Effect of carbon graphite on the crystallization of andalusite: application to the synthesis of mullite and the improvement of refractory quality, Mater. Sci. Appl. 04 (06) (2013) 10.
[19] C. Sadik, I.-E. El Amrani, A. Albizane, Recent advances in silica-alumina refractory: a review, J. Asian Ceram. 2 (2014) 83–96.
[20] A. El Haddar, E. Gharibi, A. Azdimousa, N. Fagel, I.-E. El Amrani El Hassani, M. El Ouahabi, Characterization of halloysite (North East Rif, Morocco): evaluation of its suitability for the ceramics industry, Clay Miner. 53 (2018) 65–78.
[21] A.G.M. Othman, N.M. Khalil, Sintering of magnesia refractories through the formation of periclase–forsterite–spinel phases, Ceram. Int. 31 (2005) 1117–1121.
[22] J. Anggono, Mullite ceramics: its properties structure and synthesis, J. Teknik Mesin. 7 (2005) 1–10.
[23] J.A. Pask, A.P. Tomsia, Formation of mullite from sol–gel mixtures and kaolinite, J. Am. Ceram. 74 (1991) 2367–2373.
[24] S. Somiya, R.F. Davis, J.A. Pask, Ceramic Transactions. Vol. 6-Mullite and mullite matrix composites, 1990.
[25] H. Schneider, K. Oka, J. Pak, Mullite and Mullite Ceramics, John Wiley and Sons, Chichester, England, 1994, pp. 105–145.
[26] K. Okada, Activation energy of mullitization from various starting materials, J. Eur. Ceram. 28 (2008) 377–382.
[27] C. Sadik, I.-E. El Amrani, A. Albizane, Processing and characterization of alumina–mullite ceramics, J. Asian Ceram. 2 (2014) 310–316.
[28] U. Ekpunobi, S. Agbo, V. Ajiwe, Evaluation of the mixtures of clay, diatomite, and sawdust for production of ceramic pot filters for water treatment interventions using locally sourced materials, J. Environ. Chem. Eng. 7 (2019) 102791.
[29] V. Letelier, E. Tarela, P. Muñoz, G. Moriconi, Assessment of the mechanical properties of a concrete made by reusing

both: Brewery spent diatomite and recycled aggregates, Constr. Build. Mater. 114 (2016) 492–498.
[30] F. Negró, Exhumation des roches métamorphiques du Domaine d'Alboran: étude de la chaîne rifaine (Maroc) et corrélation avec les Cordillères bétiques (Espagne) in Paris, vol. 11, 2005.
[31] F. Negro, P. Agard, B. Goffé, O. Saddiqi, Tectonic and metamorphic evolution of the Temsamane units, External Rif (northern Morocco): implications for the evolution of the Rif and the Betic–Rif arc, J. Geol. Soc. 164 (2007) 829–842.
[32] G. Suter, Carte géologique du Rif, 1/500 000, Notes Mém, Serv. géol. Maroc. 245 (1980).
[33] A. Jeannette, C. Hamel, Présentation géologique et structurale du Rif Oriental, Min. Géol. Rabat. 14 (1961) 7–16.
[34] E.A. Hilali, A. Jeannette, Kaolin et Argiles Céramiques, in: Roches et Minéraux Industriels. N° 49, numéro spécial publié par Le Ministère d'Energie et des Mines du Maroc, 1981, pp. 44–47.
[35] S. Touggant, Synthèse de la recherche des sables siliceux de Maroc, Rapport SEGM/SRIG. N° 1183, Rabat (1992).
[36] A. Manni, A. Elhaddar, A. El Bouari, I.-E. El Amrani El Hassani, C. Sadik, Complete characterization of Berrechid clays (Morocco) and manufacturing of new ceramic using minimal amounts of feldspars: economic implication, Case Stud. Constr. Mater. 7 (2017) 144–153.
[37] H. Cook, P. Johnson, J. Matti, I. Zemmels, IV. Methods of sample preparation, and X-ray diffraction data analysis, X-ray mineralogy laboratory, Deep Sea Drilling Project, University of California, Riverside. Initial reports of the deep sea drilling project, vol. 25, 1975.
[38] T. Boski, J. Pessoa, P. Pedro, J. Thorez, J. Dias, I.R. Hall, Factors governing abundance of hydrolyzable amino acids in the sediments from the NW European Continental Margin (47–50 N), Prog. Oceanogr. 42 (1998) 145–164.
[39] D.M. Moore, R.C. Reynolds, X-ray Diffraction and the Identification and Analysis of Clay Minerals, Oxford Univ Press, Oxford, 1989.
[40] G. Brown, X-ray Diffraction Procedures for Clay Mineral Identification. Crystal Structures of Clay Minerals and Their X-ray Identification, 1980, pp. 305–359.
[41] N. Fagel, E. Thamo-Bozso, B. Heim, Mineralogical signatures of Lake Baikal sediments: sources of sediment supplies through Late Quaternary, Sedim. Geol. 194 (2007) 37–59.
[42] ASTM C373-88, Standard Test Method for Water Absorption, Bulk Density, Apparent Porosity and Apparent Specific Gravity of Fired Whiteware Products, vol. 15, Annual Book of ASTM Standards, 2006, pp. 02.
[43] C. Sadik, I.-E. El Amrani, A. Albizane, Composition and refractory properties of mixtures of Moroccan silica-alumina geomaterials and alumina, New J. Glas. Ceram. 3 (2013) 59.
[44] ASTM C674-88, Standard Test Methods for Flexural Properties of Ceramic Whiteware Materials, Annual Book of ASTM Standards. 15 (2006) 02.
[45] ASTM C326-03, Standard Test Method for Drying and Firing Shrinkages of Ceramic Whiteware Clays, vol. 15, Annual Book of ASTM Standards, 2006, pp. 02.